Instrument Science Report STIS 98–22

Cosmic Ray Rejection in STIS CCD Images

Dick Shaw and Phil Hodge
June 19, 1998

ABSTRACT

We describe the method of noise model-based cosmic ray (CR) rejection in multiple, registered images, and discuss its implementation in the context of the STIS calibration pipeline. We focus on the method by which the various contributions to the uncertainty in the final, calibrated image should be combined. Unfortunately, the current design of the CR rejection module, calstis2, makes it difficult to apply the rejection threshold(s) correctly while also combining the uncertainties appropriately. We offer a solution to the problem, in the form of characterizing the uncertainties of the various calibration reference files with keywords in the science image header. We also characterize the properties of CRs in STIS CCD images, and describe the means by which the CR rejection parameters are optimized for pipeline processing. We conclude with a summary of recommendations for improving the calstis2 module and/or the corresponding off-line task, ***ocrreject****.*

1. Introduction

Cosmic rays (CRs) compromise the science that can be obtained with the STIS CCD in much the same way as with other similar, space-based instruments. The incidence of cosmic rays in near-Earth, space-based CCD detectors (outside the SAA) is ~two orders of magnitude higher than that encountered for ground-based detectors—a rate so high that special observing strategies have been developed to ameliorate the effect. For STIS, the recommended procedure (for observations of more than several minutes) is to obtain two or more exposures with identical pointing so that an anti-coincidence technique can be used in the data calibration pipeline (or in down-stream analysis) to detect and eliminate the CRs. The basic algorithm used in **calstis** (specifically, the module *calstis2*) was described by Shaw et al. (1998). Note that the functionality of *calstis2* is implemented in the off-line STSDAS task **ocrreject**.

In this ISR we describe the strategy for rejecting cosmic rays in the STIS pipeline, and show how that strategy is reflected in the *calstis2* control parameters that are stored in the

Cosmic Ray Rejection (CRR) parameters reference table. We also discuss how uncertainties in the input images and calibration reference files should be combined and propagated to the output data products. We offer some insight into certain failure modes for *calstis2*, and conclude with a number of ways in which CR rejection with error propagation will be improved in the STIS pipeline and in **ocrreject**.

2. Noisemodel-Based CR Rejection

The **calstis** pipeline uses a variation of the κ-σ clipping technique with multiple rejection cycles to identify outliers in a set of well-registered images. Here, σ is the uncertainty in the detected response, and κ is a user-settable parameter. The variation in the technique is that σ can be accurately predicted with a simple noise model, as opposed to determining it from the data, so that outliers can be identified with as few as two images. This approach has been successfully applied to WF/PC images (Shaw & Horne 1992). The technique assumes that the properties of the detector and the astronomical image have not changed between the exposures. This assumption is usually quite good for a sequence of CCD exposures of non-variable fields.

Basic 2-D Calibration

To see the effect of CR rejection in the calibration pipeline, it is useful to review the calibration steps. For the following discussion, R_k denotes the k^{th} raw image after correction for the bias offset, and the images *B, D,* and *F* correct for the residual bias structure, the dark current, and the flat-field variations, respectively. We have the following expression for the calibrated image *C* from *N* constituent (i.e., `CR-SPLIT`) images:

$$C = \frac{\sum_{k=1}^{N} (R_k - B - t_k \cdot D)}{F} \qquad \text{(Eq 1)}$$

The correction for the bias and dark can be moved outside the sum, which is more akin to the way the operations are currently performed in the **calstis** pipeline. Provided no pixels are rejected during image combination (see below):

$$C = \frac{\sum_{k=1}^{N} R_k - N \cdot B - T \cdot D}{F} \qquad \text{(Eq 2)}$$

The total exposure time, *T,* is the sum over the (potentially different) exposure times, t_k, of the constituent images:

$$T \equiv \sum_{k=1}^{N} t_k$$

Error Propagation

An expression for the uncertainty in the calibrated image can be obtained by differentiating Eq. (2) and combining the partial differentials in quadrature:

$$(\Delta C)^2 = \frac{\sum_{k=1}^{N} (\Delta R_k)^2 + (N \cdot \Delta B)^2 + (T \cdot \Delta D)^2}{F^2} + \left(C \cdot \frac{\Delta F}{F^2} \right)^2 \qquad \text{(Eq 3)}$$

Here ΔR_k is the uncertainty in the kth raw image, and ΔB, ΔD and ΔF are the uncertainties in the bias, dark, and flat-field correction images, respectively. Note that $(\Delta B)^2$ is scaled by the square of the number of images (rather than by N) since the same correction is applied to all images (i.e., the applied bias correction is not independent for each image.) Similar arguments apply for $(\Delta D)^2$, although it is scaled by the exposure time, and $(\Delta F)^2$. The noise model gives the uncertainty (in DN) at each pixel (i, j) in the raw image:

$$(\Delta R(i, j)_k)^2 = \left(\frac{N_{\text{Read}}}{G} \right)^2 + \frac{R_k'(i, j)}{G} + (N_{\text{Scale}} \cdot R_k'(i, j))^2 \qquad \text{(Eq 4)}$$

Here, N_{Read} is the read noise in electrons, G is the gain in electrons/DN, N_{Scale} is the "scale" noise, and $R'_k(i, j)$ is the raw image after correction for the residual bias: $R_k'(i, j) \equiv R_k(i, j) - B(i, j)$. Note that this expression does not account for uncertainties in the gain and read noise.

Rejection of Outliers

For CR rejection based on a noise model, the appropriate place for CR rejection to occur is after the residual bias image correction, but before the correction for dark current. This is because the thermal electrons have the same noise properties as those that record the illumination by photons, but counts from the image bias do not.

In general the computation of the calibrated image and of the error estimate are more complicated because of the need to mask known bad pixels and to reject outliers, specifically cosmic rays, from the constituent images during combination. When one or more values in a given pixel are rejected, the incomplete sum (i.e., the first term in Eq. 2) must be scaled by a factor τ back to the total integration time, where:

$$\tau = \frac{T}{T - \sum t_{\text{rej}}}$$

The sum is over the exposure times in all constituent images where a value has been rejected. This scaling gives rise to a subtlety when one or more outliers must be rejected, in that the correction for the bias image in Eq. (2) must be scaled as $(N - N_{\rm rej}) \equiv N_{\rm NR}$ rather than by τ. These scale factors will differ when the exposure times of the constituent images differ.

There is a further complication to rejecting CRs in real images, in that the sky background in broad-band imaging or slit-less spectroscopic modes can vary by a factor of up to a few during the course of a `CR-SPLIT` series (Shaw, Reinhart, & Wilson 1998). In order to distinguish outliers in a variable background at low levels, the sky level for each image (generally determined globally from the mode) must be subtracted before CRs are identified. Of course, the sky from the non-rejected images must be restored before flat-fielding the final summed, calibrated image. The more general expression at each pixel (i, j) for the combined, CR-rejected, calibrated image is:

$$C(i,\,j) \;=\; \frac{\left[\left(\sum_{k\,=\,1}^{N} \left(R_{k,\,\mathrm{NR}}(i,\,j) - B(i,\,j) - s_k\right)\right) \cdot \tau + S\right] - T \cdot D(i,\,j)}{F(i,\,j)} \qquad \text{(Eq 5)}$$

where $R_{k,NR}(i, j)$ denotes a contribution from a non-rejected image at pixel (i, j), and S is the sum of the scalar sky values, s_k, from all the individual images:

$$S \;=\; \sum_{k\,=\,1}^{N} s_k$$

The expression in Eq. (5) accounts correctly for the sky and bias image corrections even when pixels are rejected. The uncertainty corresponding to Eq. (5) follows from Eq. (3), except that the uncertainty from the non-rejected pixels must be scaled appropriately:

$$(\Delta C)^2 \;=\; \frac{\left[\sum_{k\,=\,1}^{N} \left(\Delta R_{k,\,\mathrm{NR}}\right)^2\right] \cdot \tau^2 + \left(N_{\mathrm{NR}} \cdot \Delta B\right)^2 + \left(T \cdot \Delta D\right)^2}{F^2} + \left(C \cdot \frac{\Delta F}{F^2}\right)^2 \qquad \text{(Eq 6)}$$

3. Outlier Rejection in Calstis

The rejection of CRs in **calstis** is performed in the module *calstis2* which, in the current version (V1.8, May 1998), is called just after the bias level correction but before the correction for residual bias image. (See the control flow for basic, 2-D image reduction within **calstis** in Figure 1 of Shaw et al. 1998.) The choice of this place in the calibration flow, while not ideal for CR-rejection, followed from the design requirement that the functionality of *calstis2* be isolated from the rest of the pipeline flow so that it could be

independently packaged in the off-line task **ocrreject**. In this way, CR-rejection can be invoked somewhat more flexibly (within or outside of the pipeline), at the same point or perhaps somewhat later in the flow—even after flat-fielding. The implication of isolating *calstis2* from the rest of basic 2-D calibration is that no knowledge of the reference files (including the residual bias, dark, or flat-field correction images and the corresponding uncertainty arrays) is permitted, save for the CR rejection parameters table.

The current design of *calstis2* presents somewhat of a dilemma, as can be seen by referring to Eqs 5 and 6. Placing CR rejection before subtracting the residual bias image means that B will be improperly scaled if the exposure times are different (so that C will be incorrect by a small amount). In addition, the κ-σ rejection threshold would be incorrect by a small amount at count rates well above the read noise because of the improper contribution of the residual bias to the raw images. On the other hand, if CR rejection were placed after bias image correction then the scaling for outliers would be correct even if the exposure times are different, and the rejection threshold would be correct too. But the uncertainty from the bias image would contribute as N, rather than N^2, since it would have been combined with that of each raw image before calling *calstis2*. This problem of improperly scaling the various error contributions is exacerbated if CR rejection is performed even later in the calibration processing: after dark or flat-field correction—which is where CR-rejection for most other CCD data (e.g., WFPC-2 images) is invoked.

The essence of the current dilemma in *calstis2* is how to perform CR-rejection at the appropriate place in the pipeline, with a minimum of information about the various calibration reference files, while still providing a mechanism for distinguishing the various contributions to the uncertainty array. We note that the uncertainties in the reference files are typically small compared to the minimum for the individual images (~4 electrons for `ATODGAIN=1`). In fact, for the most recently delivered CCD reference files, ΔB ~0.4, ΔD~1.6x10^{-3} (though this contribution will exceed the read noise for exposures exceeding 42^{m} duration), and ΔF~7x10^{-3}. In this limit, it may be reasonable to approximate the uncertainties in these quantities with global values. These values could be stored as parameters in the image header, with an initial value of zero, and would be updated by the *calstis1* module at the time the correction is being applied. By further assuming that, on average, $F^2 = \langle F \rangle^2 = 1$ it is possible to use Eq. (6) to disentangle (at least approximately) the various error sources during image combination. That is, *calstis2* would have enough information to remove the contributions to the R_k uncertainty arrays from the bias, dark, and flat-field reference files (if these corrections have been applied) before the ERR array for the combined image is computed. If one or more of the corrections have not been applied, then the corresponding keywords (`BIASERR`, `DARKERR`, `FLATERR`) will have the value zero, and the error propagation will reflect that. Of course, for the reasons cited above, the calculation of the calibrated image C will, strictly speaking, be most correct if CR rejection follows bias image correction and precedes the dark correction.

4. Properties of CRs in STIS Images

The properties of CRs in STIS CCD images have been studied in dark calibration images and in science images. The dark frames were taken as a part of SMOV program 7085, and consisted of thirteen exposures of 15^m duration each. They provide the most accurate measurement of the CR rates and the best characterization of the CRs themselves, while the science images provided valuable information on the practicalities of outlier rejection in the presence of astronomical targets with various illumination levels. The incidence of pixels in a series of dark exposures that were affected by CRs, as a function of clipping threshold, is shown in Fig. 1. The number of outliers that would be expected from a normal distribution is shown for comparison. The most interesting feature is that the most deviant values (the ones we associate with a CR event) are detected easily, and that the number of affected pixels is a surprisingly insensitive function of the rejection threshold. That is, ~75% of pixels affected by CRs are detected with a 6σ threshold, and 87% are detected with a 4σ threshold; a 3σ threshold will exclude nearly all CR-impacted pixels.

Figure 1: Number of pixels identified as outliers in an exposure (normalized to 1000 s) as a function of rejection threshold in units of standard deviation (σ). The total of the outliers (*solid curve*) is comprised of genuine CRs (*dashed curve*) and deviations that would be expected in a normal distribution (*dotted curve*).

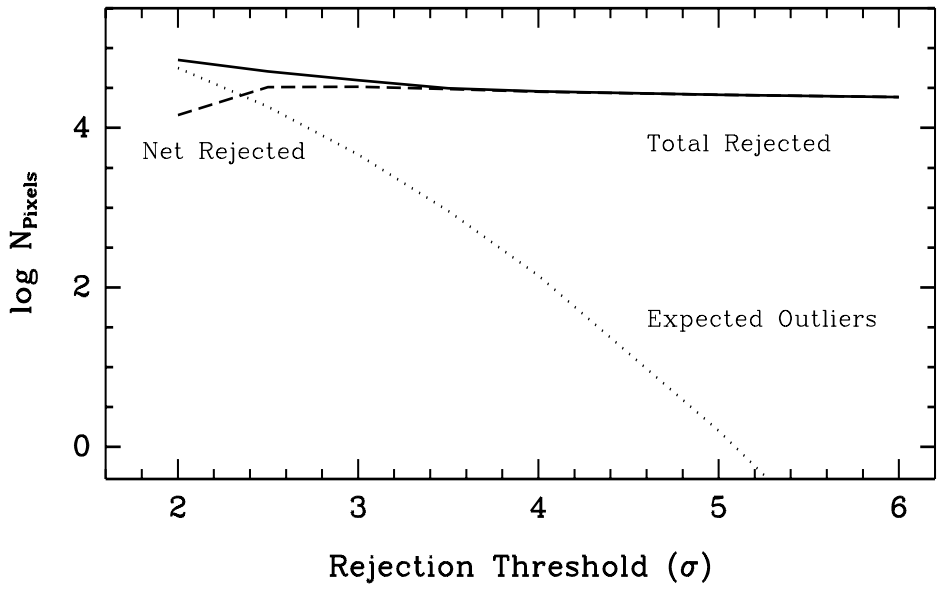

Using a 3σ rejection threshold, we find that CRs affect STIS CCD images obtained outside the SAA at a rate of 32 pixels/s over the whole detector, with a variation of ~20%. Each CR event typically affects 6–10 pixels, though many tens of pixels can be affected for grazing-incidence CRs. This rate is ~1 CR/s/cm^2, which is in relatively good agreement with the rate observed for WFPC-2 outside the SAA.

Optimization of Rejection Parameters

Important as it is to remove the effect of CRs from data analysis, it is even more important not to corrupt the character of the underlying data in the process. Most analysis applications in use today for CCD data have the ability to compute an estimate of the uncertainty associated with parameterized fits to physical or empirical models of the flux distribution. These utilities generally assume some sort of model for the noise, and that the underlying counts obey a Gaussian or Poisson distribution. Thus, it is important not to violate these assumptions by setting too restrictive a rejection threshold, and thereby artificially conditioning the data.

The rejection parameters must also be adjusted according to the mean exposure time to reflect the expected incidence of CRs, and to ameliorate the effect of coincident CRs. It is not useful to set a global threshold such that the number of expected outliers would exceed the number of CR-impacted pixels. For example, ~140 pixels in a single image would be expected to deviate from the "truth" image by more than 4σ. If images are affected by CRs at a rate of 32 pixels/s, we would not expect 140 CR-impacted pixels for single exposures of less than ~4.4 s duration. The exposure time needed for CR-impacted pixels to equal that for a given, minimum rejection threshold is shown in Fig. 2. Note that the required total exposure time scales as the number of images, *N*, in repeated exposures.

Figure 2: Total exposure time needed for the number of CR-impacted pixels to equal that expected by imposing a rejection threshold on a normal distribution, assuming a CR rate affecting 32 pixels/s, for a single image (*solid curve*) and for multiple images (*dotted curve*, for N=8) if the exposure is repeated or is `CRSPLIT`.

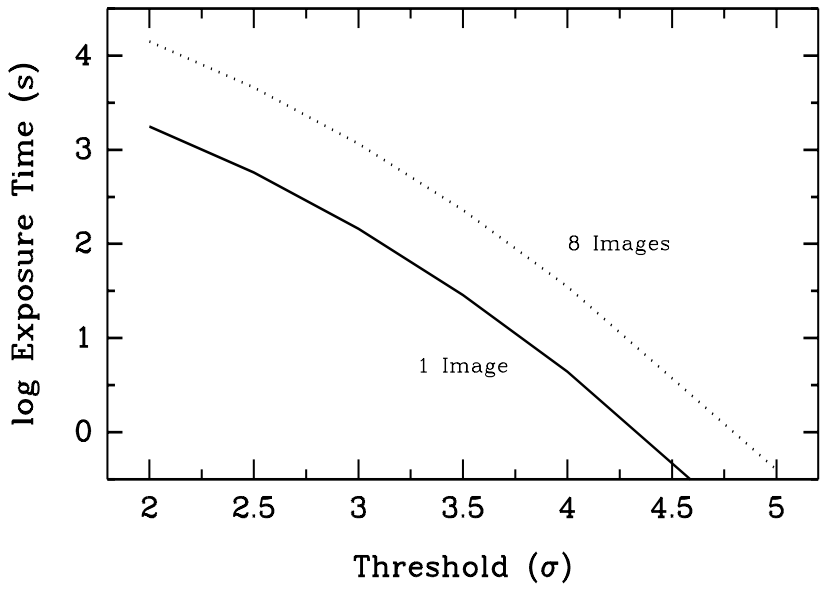

It is possible to reject selectively outliers caused by CRs with a tighter threshold than that implied in Fig. 2 by lowering the threshold for pixels spatially adjacent to locations where a CR has been identified. This "sympathetic rejection" takes advantage of the fact

that CRs tend to affect multiple, neighboring pixels. This approach has been validated in science exposures of the Hubble Deep Field-South, where a simple rejection at the 5σ level leaves rings of residual, low-level charge around pixels where CRs have been eliminated (Ferguson 1998, private communication). In this case, setting the rejection threshold for neighboring pixels at 2.5σ eliminated the problem.

At the other extreme, the high rate at which pixels are affected by CRs means that the probability of coincident CRs cannot be ignored for sufficiently long exposures. The probability that any given pixel in an image will be affected by a single cosmic ray during an exposure is:

$$P_1 = \frac{R \cdot \Delta t}{N_{\rm pix}} \qquad \text{(Eq 7)}$$

where R is the rate at which pixels are affected by CRs, Δt is the exposure duration, and $N_{\rm pix}$ is the number of pixels in the image. The probability that two CRs will affect a given pixel, assuming the individual probabilities are independent, is just the product of the individual probabilities. If we choose a maximum tolerable probability of coincident CRs, then Eq. (7) can be re-written to give the maximum total exposure time:

$$\Delta t = \frac{\sqrt{P_1 \cdot P_2}}{R} \times N_{\rm pix} \qquad \text{(Eq 8)}$$

This relation can be generalized to a larger number of coincident CRs by taking the n^{th} root of the product of the individual probabilities. If the probability of two coincident CRs is to be kept smaller than 0.01% per pixel, given a rate of 32 pixels/s that are affected by CRs over a 1024x1024 image, Eq. (8) implies an exposure time of 328s, or ~5.5 minutes. Observers may be more tolerant of coincident CRs for some programs, particularly spectral programs and/or when read noise limits the achievable signal-to-noise. But in general a `CR-SPLIT` >2 should be considered whenever possible for CCD exposures longer than ~$10^{\rm m}$, and a `CR-SPLIT` of 3 or 4 for full-orbit exposures.

The following points summarize the strategy for optimizing the CR rejection parameters for the STIS pipeline:

- The rejection threshold should generally be set no lower than 3σ, and preferably 4σ. If “sympathetic rejection” is enabled, the threshold for neighboring pixels should be no lower than 2.5σ.
- The sky background should always be removed for good CR rejection at low illumination levels.
- Use the median of the scaled images as the initial guess of the “truth” image, unless reject cycles are used.
- Use multiple rejection cycles if the mean exposure time is such that the probability of coincident CRs exceeds 0.01%.

The recommended parameter combinations for a new CRR reference table are summarized in the Appendix. Note that the GOs can and should vary these parameter settings in the off-line environment to achieve the best results for their science.

Caveats

In spite of the robustness of noise model-based CR rejection, there are some circumstances where the implementation in *calstis2* will fail. The most severe failures will occur when combining images that are not well registered (i.e., to within ~0.1 pixel). The reason for this is that the spatial FWHM for unresolved point sources is ~2 pixels. This effect is illustrated in Fig. 3 for spectral image o3tt40040, which is a portion of a G750L spectrum of a calibration standard. The four `CR-SPLIT` frames in this 30^{m} exposure were mis-registered by as much as 0.3 pixel in the spatial direction. Since the width of the PSF is so narrow this lead to valid data being rejected when the frames were combined.

Figure 3: Portion of a spectrum of the standard star GD153, which was a 30 min, `CR-SPLIT=4` exposure with G750L. The effect of CR rejection on these mis-registered frames is most evident in the dark, horizontal line near the center of the stellar profile, where all data were rejected as outliers.

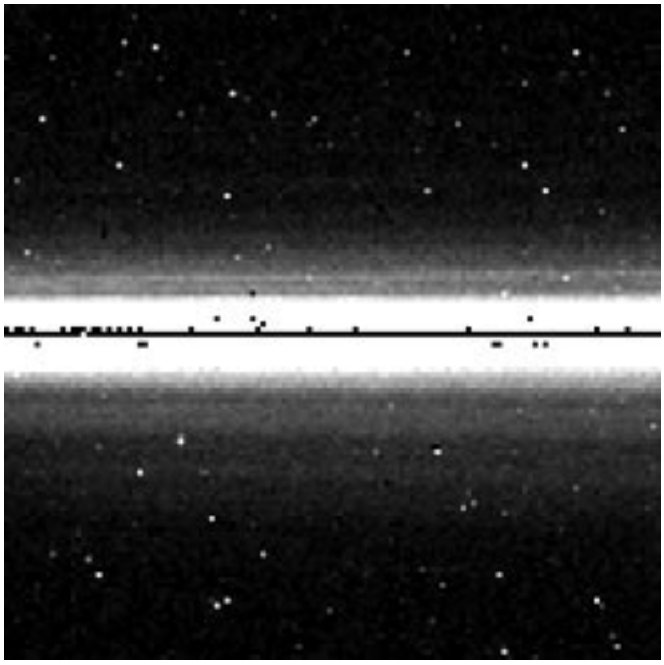

The spatial profiles of two of the frames, along with that of the combined frame, are shown in Fig. 4. All data were rejected at the center of the profile because *calstis2* rejected on both the low and high side from the initial guess image, which was the median of the individual frames. This problem can be ameliorated by setting the `INITGUES` parameter to “minimum” and using rejection cycles, although valid data will still be rejected unless the rejection thresholds are set fairly high. Although an option is planned for *calstis2* to reject solely on the high side (which would focus more precisely on rejecting CRs), we

note that rejection on the low side would be needed for combining images that have been spatially dithered. Support in *calstis2* (or more likely, the off-line task **ocrreject**) for combining dithered images would be very useful for programs that require higher S/N ratios than the available flat-fields can support, or that need the greatest possible spatial resolution, since the STIS CCD pixels are slightly larger than that needed for critical sampling. However, such an enhancement of **ocrreject** would have to involve some sort of image resampling to identify CRs if the dither offsets are not even multiples of the pixel size.

Figure 4: The spatial profiles of the first and last frames in image o3tt40040, superimposed on the (scaled) profile of the combined frame.

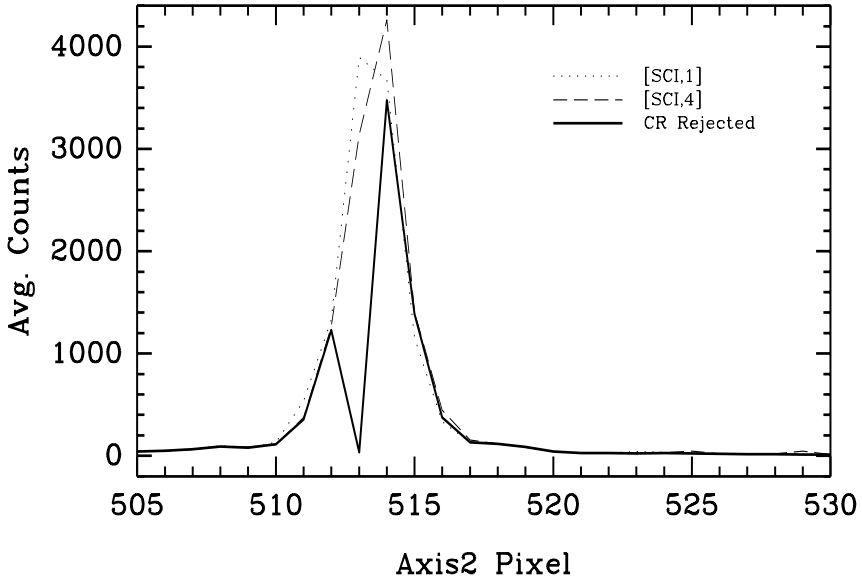

One other, minor caveat involves the use of the image mode for determining the sky background. Generally, it can be challenging to determine an accurate estimate of the mode for a set of floating-point values, and the accuracy is limited by the choice of the bin size for the histogram, and the method for refining the initial estimate after the approximate mode has been found. It is also possible, with certain illumination patterns on the image, for the image histogram to be bi- or multi-modal. In this case, it is possible that different modes will be selected as the sky value on one or more of the CR-split images. These conditions are probably rare, but this possibility should be kept in mind if the CR rejection appears to have yielded poor results.

5. Summary of Planned Enhancements

The **calstis** pipeline, in the module *calstis2*, is capable of robustly rejecting cosmic rays from CCD data, while generally not compromising the scientific content. However, there are ways in which the pipeline can be improved to better reject CRs in some cases, and in all cases to improve the estimate of the uncertainty in the calibrated image. Specifically, the following enhancements are planned for *calstis2* and **ocrreject**:

- In the **calstis** pipeline, place CR rejection after correction for the residual bias image, but before correction for the dark current.
- Put global estimates of the mean error for each of the bias, dark, and flat-field reference images in the header of all science images, in the keywords `BIASERR`, `DARKERR`, and `FLATERR`. These values should be initialized to zero, and should be populated by the module *calstis1* after each step is performed.
- C*alstis2* will be upgraded to properly account for the contribution to the error from the bias, dark, and flat-field calibration steps, as characterized in the new keywords.
- "Sympathetic rejection" in neighboring pixels will be implemented in the pipeline, although the rejection threshold for neighboring pixels should be no tighter than 2.5σ.
- Only deviant values on the high side of the mean need be rejected, except when combining images that have been spatially dithered, and *calstis2* will be enhanced to support that as an option.
- Either *calstis2* or **ocrreject** should eventually be upgraded to support CR rejection in dithered images, at least for the case were the dither offsets are even multiples of the pixel size.

References

Shaw, R., & Horne, K. 1992, *Noise Model-Base Cosmic Ray Rejection for WF/PC Images*, in ASP Conf. Ser., Vol 25, *Astronomical Data Analysis Software & Systems I*, eds. D. Worrall, C. Biemesderfer, & J. Barnes (San Francisco, ASP), p. 311

Shaw, R., et al. 1998, *Calstis2: Cosmic Ray Rejection in the STIS Calibration Pipeline*, STIS Instrument Science Report ISR 98–11

Shaw, R., Reinhart, M, & Wilson, J. 1998, *Scattered Light from the Earth Limb Measured with the STIS CCD*, STIS Instrument Science Report ISR 98–21

Appendix: CR-Rejection Parameters for Calstis

Table 1 below gives the rejection parameters for *calstis2* that implement the strategy outlined in §4 above. The format of the table, and the interpretation of the parameters, was described by Shaw, et al. (1998). The major differences between this table and the most recently delivered CRR reference table are:

- The choices of `MEANEXP` have been updated to reflect the correct variation of minimum threshold with the number of exposures to be combined (c.f. Fig. 2).
- The use of somewhat higher rejection thresholds (generally 4σ vs. 3σ), but a minimum 3σ threshold for pixels bordering a detected CR.
- A change of the `INITGUES` parameter to use the minimum when rejection thresholds are invoked, rather than the median value, as the initial estimate of the "truth" image. This is necessary until *calstis2* has an option to reject solely on the high side.

Table 1. Revised settings for STIS Cosmic Ray Rejection Parameters (CRR) reference table.

CRSPLIT	MEANEXP	INITGUES	SKYSUB	CRSIGMAS	SCALENSE	CRRADIUS	CRTHRESH	BADINPDQ	CRMASK
2	4.4	minimum	mode	5	0.	1.5	0.80	0	yes
2	28.6	minimum	mode	4	0.	1.5	0.875	0	yes
2	145.	minimum	mode	4	0.	1.5	0.75	0	yes
2	3.0E5	minimum	mode	4	0.	1.5	0.75	0	yes
3	4.4	median	mode	5	0.	1.5	0.80	0	yes
3	28.6	median	mode	4	0.	1.5	0.875	0	yes
3	145.	median	mode	4	0.	1.5	0.75	0	yes
3	328.	minimum	mode	5,4	0.	1.5	0.75	0	yes
3	3.0E5	minimum	mode	5,4	0.	1.5	0.75	0	yes
4	4.4	median	mode	5	0.	1.5	0.80	0	yes
4	28.6	median	mode	4	0.	1.5	0.875	0	yes
4	145.	median	mode	4	0.	1.5	0.75	0	yes
4	328.	minimum	mode	5,4	0.	1.5	0.75	0	yes
4	1521.	minimum	mode	5,4	0.	1.5	0.75	0	yes
4	3.0E5	minimum	mode	5,4	0.	1.5	0.75	0	yes
5	4.4	median	mode	5	0.	1.5	0.80	0	yes
5	28.6	median	mode	4	0.	1.5	0.875	0	yes
5	145.	median	mode	4	0.	1.5	0.75	0	yes
5	328.	median	mode	4	0.	1.5	0.75	0	yes
5	1521.	minimum	mode	5,4	0.	1.5	0.75	0	yes
5	3.0E5	minimum	mode	5,4	0.	1.5	0.75	0	yes
6	4.4	median	mode	5	0.	1.5	0.80	0	yes
6	28.6	median	mode	4	0.	1.5	0.875	0	yes
6	145.	median	mode	4	0.	1.5	0.75	0	yes
6	328.	median	mode	4	0.	1.5	0.75	0	yes
6	1521.	minimum	mode	5,4	0.	1.5	0.75	0	yes
6	3277.	minimum	mode	5,4	0.	1.5	0.75	0	yes
6	3.0E5	minimum	mode	5,4	0.	1.5	0.75	0	yes
7	4.4	median	mode	5	0.	1.5	0.80	0	yes
7	28.6	median	mode	4	0.	1.5	0.875	0	yes
7	145.	median	mode	4	0.	1.5	0.75	0	yes
7	328	median	mode	4	0.	1.5	0.75	0	yes
7	1521	median	mode	4	0.	1.5	0.75	0	yes
7	3277	minimum	mode	5,4	0.	1.5	0.75	0	yes
7	3.E5	minimum	mode	6,5,4	0.	1.5	0.75	0	yes
8	4.4	median	mode	5	0.	1.5	0.80	0	yes
8	28.6	median	mode	4	0.	1.5	0.875	0	yes
8	145.	median	mode	4	0.	1.5	0.75	0	yes
8	328.	median	mode	4	0.	1.5	0.75	0	yes
8	1521.	median	mode	4	0.	1.5	0.75	0	yes
8	3277.	minimum	mode	5,4	0.	1.5	0.75	0	yes
8	3.E5	minimum	mode	6,5,4	0.	1.5	0.75	0	yes